Effect of Magnetic Field on Calcium - Silica Fouling and

Interactions in Brackish Water Distribution Systems

Zeyuan Liu [a,b], Marco Di Luccio [c], Sergio García [d], Jaume Puig-Bargués [e], Xiao Zhao [a,b], Alfredo

Trueba [d], Tahir Muhammad [a,b], Yang Xiao [a,b], Yunkai Li [a,b*]

[a.]College of Water Resources and Civil Engineering, China Agricultural University, Beijing 100083, China

[b.]Engineering Research Center for Agricultural Water-Saving and Water Resources, Ministry of Education, Beijing 100083, China

[c.]Department of Chemical and Food Engineering, Federal University of Santa Catarina, Florianópolis, SC, Brazil

[d.]Department of Sciences & Techniques of Navigation and Shipbuilding, University of Cantabria, C/ Gamazo 1, 39004 Santander, Spain

[e.]Department of Chemical and Agricultural Engineering and Technology, University of Girona, Girona 17003, Spain.

[1]

---

[1] Corresponding author at College of Water Resources and Civil Engineering, China Agricultural University, Beijing

100083, China

E-mail: yunkai@cau.edu.cn (Yunkai Li)

13   **Abstract**:

14   Fouling growth in brackish water distribution systems (BWDS), especially calcium-silica fouling, is

15   inevitable issue in brackish water desalination, chemical and agricultural industry, eventually threaten

16   the cleaner production process and environment. Magnetic Field (MF) has been a greener and effective

17   technology to control calcium carbonate fouling. However, the effects of MF on composite calcium-silica

18   fouling are still elusive. Therefore, this paper assessed the effect of MF on calcium and silica fouling. We

19   found that MF not only significantly reduce the calcium carbonate fouling, but also obviously decreased

20   the silica fouling. The MF reduced the calcite fouling reached 38.2%-64.3% by changing water quality

21   parameters to trigger the transformation rate of $CaCO_3$ crystal from compact calcite to looser aragonite,

22   as well as increase the unit-cell parameters and chemical bond lengths of calcite and aragonite. The MF

23   also decreased the content of silica fouling (silica and silicate) reached 22.4-46.3% by reducing the

24   concentration of soluble silica and accelerating the flocculation settlement to form large size solid

25   particles in BW. Furthermore, MF broke the synergistic interactions among calcium and silica fouling.

26   In addition, the anti-fouling ability of permanent MF was higher by 12.3-35.1% than electric MF. Overall,

27   these findings demonstrate that MF is an effective and chemical-free technology to control calcium-silica

28   fouling in BWDS, and provide a new perspective for sustainable application of brackish water.

29   **Keywords**: fouling control; calcium fouling; silica fouling; permanent magnetic field; electric magnetic

30   field

31

32

1 Introduction

Fresh water scarcity will be the world major crisis in future few decade (Hanikel et al. 2020). The effective application of brackish water (BW) could be an important means to alleviate local crisis of fresh water resources, and has been gradually become major component of global water sustainable management (Aliaskari and Schafer 2021, Guo et al. 2019). However, BW contained various soluble salts and suspended colloidal particles, leading to calcium carbonate and silica fouling in water distribution systems, heat exchangers and membranes (Chang et al. 2021, German et al. 2019, Park et al. 2019). Particularly in agricultural water distribution systems, the presence of fouling would reduce the irrigation and fertilization uniformity (Ma et al. 2020, Muhammad et al. 2021), aggravates the salinization of farmland and excessive use of fertilizer, resulting in environmental hazardous issues (Zhang et al. 2021). Chemical treatments are the most common methods to mitigate fouling in BW distribution systems (Al-Sabagh et al. 2018, Suharso et al. 2019). However, due to risk of environmental pollution and high cost, the application of chemical reagents is limited (Greenlee et al. 2009, Song et al. 2019). Thus, an effective and green methods for mitigation of fouling in BWDS is in urgent need.

Magnetic field (MF) has attracted an extensive interest for mitigation of calcium fouling, due to its characteristics of low cost, low energy consumption, and easy-to-operate (Fathi et al. 2006, Holysz et al. 2003, Xiao et al. 2020, Zhang et al. 2017b). Wang et al. (1997) reported that MF shortened the induction period of calcium carbonate fouling and formed higher quantity of crystals with smaller sizes. Johan et al. (2016) found the MF changed the crystal formation and morphologies of calcium carbonate, promoting the transformation of calcite to aragonite with low adhesive properties, and the fouling inhibition rate were reached 46.7%. These studies brought valuable insights into the anti-fouling ability of MF. The available literature related to the anti-fouling effects of MF mainly focuses on calcium

55   carbonate fouling. However, BW not only contains plenty of fouling-forming ions i.e. Ca^{2+}, Mg^{2+}, HCO_3^-

56   (Du et al. 2020, Sriramulu et al. 2019), but also high silica concentration and silica suspended colloidal

57   particles (Nthunya et al. 2019, Shemer et al. 2019). Thus, silica fouling are also significant components

58   to fouling formation (German et al. 2019, Wang et al. 2020). In addition, calcium carbonate and silica

59   fouling are often occurred simultaneously (Antony et al. 2012, Demadis et al. 2005). However, the

60   controlling effects of MF on calcium carbonate and silica fouling in BWDS are still elusive. Moreover,

61   the strong interactions between different fouling mostly leads to the complex behaviors of fouling. For

62   instance, $CaCO_3$could provide nucleation sites for silicate (Umar et al. 2013). In other words, the

63   presence of $CaCO_3$ would promote the formation of silicates. So far, the controlling effects of MF on

64    $CaCO_3$ has been fully demonstrated. Therefore, this study assumes that MF could affect the formation of

65   silica fouling (e.g. silica, silicates) by acting on calcium carbonate, with implication for composite fouling

66   control for BWDS. However, the impacts of MF on the interactions among various fouling in BWDS

67   have not been fully understood yet.

68   The fouling in BWDS always show crystal texture. Previous studies demonstrated that MF could

69   affect the microscopic characteristics of crystals (Urusovskaya et al. 2003). It is worth noting that the

70   microscopic characteristics of crystals are closely related to the formation of crystals. For example,

71   Simunek and Vackar (2006) reported that the hardness of a crystal is determined by the microscopic

72   characteristic parameters of the crystal, such as bond strength, bond length, and ionic properties.

73   Therefore, it can be inferred that MF might control composite fouling by acting on the microscopic

74   characteristics of crystals in BWDS. However, the effects of MF on crystal microscopic characteristics

75   for fouling have not been evaluated yet.

76   Thus, the objectives of this study were to: (i) determine whether MF would effectively control the

77 fouling in BWDS; (ii) reveal the influence mechanism of MF on calcium carbonate fouling, silica fouling

78 and their interactions; and (iii) clarify the controlling effects of different types MF generation methods

79 on fouling, and propose the MF selection strategy.

80 2 Materials and methods

81 2.1 Experimental setup

82 The testing system was an outdoor-designed fouling cultivation platform (Fig. 1). The platform

83 resembles agricultural BDWS, with four layers of drip irrigation pipelines stacked horizontally. Each

84 layer had the same type of emitter. A total of four types of emitters were subjected for fouling cultivation,

85 being their structural parameters shown in Table S1. Each layer contained eight 15 m long drip irrigation

86 pipelines with 45 identical emitters evenly spaced along each pipeline. Emitters due to their narrow

87 (between 0.5-1.2 mm) flow channels, are the suitable place for fouling and consequently leads to the

88 system clogging. The experiment lasted for a total of 440 hours, with daily system operation of 14 hours

89 (7:00 am-9:00 pm). The BW used in the experiment was collected from the local surface lake (located in

90 northern Wulan Buh, Dengkou County, Bayan Nur City, Inner Mongolia, China). The basic quality

91 characteristics of the applied BW are listed in Table 1. The BW was temporarily stored in water tank and

92 filtered with a disc filter (106 μm), then flowed into a pipeline that contained magnetizer to obtain

93 magnetized water. The magnetized water was filtered again through a screen filter (150 μm), and then let

94 into the drip irrigation pipelines. The flow rate at the entrance of the system was maintained at 15 m^3 h^-

95 ^{1}.

96   #Fig. 1 approximately here#

97   #Table. 1 approximately here#

2.2 Experimental treatments

Two types of magnetizers were selected, including permanent magnetic field (PMF, manufacturer: Shanghai Bojian, China; type: CNF) and electric magnetic field (EMF, manufacture: Yishui, China; type: MD-63). The operational details of the PMF were: magnetic flux density measured by Gauss meter (Bell, Model 6010), 600 and 900mT; material of magnets, neodymium-iron-boron (Nd2Fe14B) magnets; placement of magnets in tube, attraction (N-S). The operational details of EMF were: working voltage, 12 V; magnetic flux density, 300 Gs; coil external diameter, 32 mm; total coil number, 40. According to the types of magnetizers, five treatments were set in the experiment: control group with no-MF (CK), permanent magnetic fields with 600mT (PMF_600mT), and permanent 900mT (PMF_900mT), electromagnetic fields with 20 kHz frequency (EMF_20kHz) and 30 kHz frequency (EMF_30kHz).

2.3 Evaluation of BWDS performance

Along with operation time, the growth of composite fouling would gradually clog the drip emitters of BWDS. The average discharge variation ratio (Dra) was used to evaluate the flow performance of BWDS. The detailed calculation method of Dra is being explained in supplementary material (section 1.2).

2.4 Water quality parameters

Previous studies demonstrated that, the MF would obviously affect the water quality characteristics (Florez et al. 2012, Garcia and Trueba 2018, Trueba et al. 2015). Since water quality is the major factor affecting the fouling formation, this paper focuses on parameters of pH, electrical conductivity (EC), oxidation reduction potential (ORP), surface tension (ST), zeta potential (Zeta), silica concentration (SC)

6

118 suspended solids (SM) and particle size distribution (PSD). Electrical conductivity (EC) and pH were

119 measured by a conductivity meter (Manufacturer: Leici, China; type: DDSJ-319L) and a pH meter

120 (Manufacturer: Mingbo, China; type: PHS-3C), respectively. Oxidation reduction potentials (ORP) were

121 tested by an ORP meter (manufacturer: Kedida, China; type: CT-8022). Surface tensions (ST) were

122 determined by a surface tensiometer (manufacturer: Huakun, China; type: DT-102A). Particle size was

123 analyzed by using a laser particle sizer (Malvern Instruments Ltd., Mastersizer 3000). Zeta potential were

124 measured by Zeta potential analyzer (Manufacturer: micromeritics, America; type: Nanoplus).

125 Suspended matter was tested by Gravimetric method according to GB 11901-89. Silica concentration

126 was tested with silico–molybdenum blue spectrophotometry method according to PN C04537-04-1988.

127 **2.4 Extraction and analysis of composite fouling in emitters**

128 During the experiment, the composite fouling in each treatment was collected for a total of eight

129 times, after every 55 h of system operation. At each sampling event, a single irrigation pipeline was

130 fetched from the testing system for each type of emitter. Each time, 18 emitters randomly selected at

131 irrigation pipelines (i.e. 6 at the head, 6 at the middle and 6 at the tail) were peeled off. The samples were

132 then placed in zip lock plastic bags and kept in refrigerator (4℃).

133 **2.5.1 Dry weights of composite fouling**

134 The fouling dry weight inside emitters was obtained eight times during system operation, at 55 h,

135 110 h, 165 h, 220 h, 275 h, 330 h, 385 h, and 440 h respectively. The obtained emitter samples were put

136 in a zip lock plastic bag. Hereafter, 20 mL of deionized water were added to these zip lock plastic bags,

137 and were put in an ultrasonic cleaning bath (manufacturer: Chaowei, China; type: GVS-10 L; working

138 power: 240 W; frequency: 60 Hz) for 60 min to remove the fouling. The mixed solid phase of the

139 sampling event acquired at the bottom was dried (100℃) to a constant weight and then weighed using a

140 high-precision electronic balance (manufacturer: Wangtai, type: FA-G; accuracy: 10^{-3} g).

2.5.3 Minerals components in composite fouling

A vacuum freeze dryer (manufacturer, Guansen, China; type, FD-A12N) was used to dry the fouling. Then, an X-ray diffractometer (XRD, manufacture: Bruker, Germany; type: D8-Advance) was used to analyze the mineral components in fouling. To obtain the lattice parameters (i.e. a, b, and c) and crystal volumes of various fouling, the Rietveld refinements of XRD were used by General Structure Analysis System (GSAS) software.

2.5.4 Crystals apparent morphology

The crystal morphological appearances were examined using scanning electron microscope (SEM, manufacturer: Japan Jeol, model: S-3400N), at an acceleration voltage of 20 kV, after sputtered with gold film, and magnification ranging from 400× to 15,000×.

2.6 Statistical analysis

The experimental data basic calculations were done in Microsoft Excel; and statistical analysis was carried out with SPSS (ver. 22.0 IBM, USA). Pearson correlation coefficient was applied to determine the correlation of mineral's content among different groups (p. adjusted <0.05). Analysis of Variance (ANOVA) was applied. Structural equation modelling analysis (SEMA) was performed using SPSS AMOS v.24 (AMOS, IBM, USA) to analyze the direct and indirect relationships among magnetic fields, mineral contents, and the flow performances of BWDS (Dra).

3 Results

3.1 Water quality, fouling components and BWDS performances

The EC, pH, ST, ORP, of applied water (Fig. 2a-d) changed obviously after the application of MF. MF decreased EC (Fig. 2a) and ST (Fig. 2c) by 0.13-0.16dS m^{-1} and 0.83-11.5mN m^{-1}; while increased the pH (Fig 2b) and OPR (Fig 2d) by 0.036-0.0832 and 7.2-31.6mv. In addition, there were obvious differences among different MF treatments. Comparing with PMF, EMF increased the EC and ST to

164   0.02-0.11dS m^{-1} and 0.592-7.69mN m^{-1}, and decreased the pH and the OPR by 0.028-0.052, 1.9-24.3mV,

165   respectively.

166   The dry weights of fouling (Fig. 2e) and BWDS performances showed that MF significantly ($p <$

167   0.01, Table S1) reduced the fouling contents by 30.2-54.8%. Consequently, MF obviously alleviated the

168   clogging of the BWDS with the Dra (Fig. 2f) significantly ($p < 0.01$, Table S2) increased by 26.5-49.7%.

169   Different MF generation methods also significantly ($p <0.01$, Table S2) influenced the clogging dry

170   weight. The two PMF treatments had higher control efficiencies of fouling than the two EMF groups.

171   Compared with EMF treatments, the fouling content in PMF groups decreased by 12.3-35.1%. Moreover,

172   the intensity in PMF treatments and the frequency in EMF groups had impacts on the anti-fouling ability.

173   It was found the fouling content in PMF_900mT group decreased by 13.6-15.2% compared with

174   PMF_600mT. the fouling content EMF_20 kHz decreased by 10.9-12.6% compared with EMF_30 kHz.

175   #Fig. 2 approximately here#

176   **3.2 Effect of MF on mineral component proportions and appearance of fouling**

177   X-ray diffraction patterns indicated a total of six different minerals appeared in composite fouling

178   (Fig. 3a): carbonates (i.e. calcite and aragonite), silicates (anorthites, chlorites, and muscovite), and silica.

179   Carbonates were formed by the chemical reactions ($Ca^{2+} + HCO_3^-=CaCO_3 +H^+$). The formation of

180   silicates and silica fouling is mainly due to the monomeric deposition, polymerization, and particle

181   accumulation of dissolved silica, colloidal silica and sand particles in water. MF influenced the

182   proportions of minerals, reducing the proportion of carbonate by 4.2-12.3%, and increasing the

183   proportion of silicate and silica by 1.5-5.2%, 2.7-7.1%, respectively (Fig. 3b).

184   The surface morphology of composite fouling (Fig. 3c) revealed by SEM indicated that the fouling

185   particles with different sizes combined closely each other, showing a complex fouling morphology. MF

9

186 treatments reduced the content of fouling on the emitter surfaces and changed their morphology. For

187 example, compared with control group, the fouling size became much smaller and distributed wider.

188   #Fig. 3 approximately here#

3.3 Effect of MF on calcium carbonate fouling

190   The dynamic changes of carbonate contents are shown in Fig. 4a, c. The results show that the MF

191 significantly ($p < 0.01$, Table S3) reduced the carbonate contents by 33.4-60.7% (Fig.S3). MF treatment

192 reduced the calcite content by 12.4-19.5 mg cm^{-2}, while increased the aragonite content by 1.3-4.2 mg

193 cm^{-2}. Significant differences ($p < 0.01$, Table S3) in carbonates content were found among different MF

194 treatments. The two PMF treatments had higher control efficiency on carbonates than the two EMF

195 treatments ($p < 0.01$, Table S3). Compared with EMF, PMF treatments decreased the carbonates content

196 by 13.5-36.6%. In addition, the intensity in PMF treatments and the frequency in EMF groups had

197 impacts on the carbonates content. Thus, the carbonates content in PMF_900mT decreased by 14.3-16.2%

198 compared with PMF_600mT, and EMF_20kHz decreased the carbonates content by 10.3-12.5%

199 compared with EMF_30kHz.

200   The cell volume and chemical bonds of carbonates (Fig. 4b, d) show that MF considerably changed

201 the crystal structure parameters of calcite and aragonite. Compared with CK treatment, the cell volume

202 (Cv) of calcite and aragonite treated by MF was considerably larger than that treated by CK with an

203 increase ratio of 11.42-43.43 Å^3 and 7.2-31.73 Å^3. Moreover, compared with CK treatment, the Ca-Ca

204 and Ca-C bonds of calcite in MF treatment all increased by 0.1-0.5% and 0.3-1.5%, the Ca-Ca and Ca-C

205 bonds of aragonite in MF treatment all increased by 0.1-0.4% and 0.3%-1.1%.

206   #Fig. 4 approximately here#

3.4 Effect of MF on silica fouling

The dynamic change of silica fouling (Fig. 5) shows that MF significantly ($p < 0.01$, Table S4) affected the contents of silicate and silica. MF reduced the contents of chlorites, muscovite, anorthite and silica by 0.97-2.44 mg cm^{-2}, 0.53-1.06 mg cm^{-2}, 0.75-1.45 mg cm^{-2}, 1.28-2.56 mg cm^{-2}, respectively, and the content of silicate and silica decreased by 21.8-47.9% and 22.7-44.3%. Significant differences ($p < 0.01$, Table S4) were found in silicate and silica contents among different MF-treatments. The two PMF treatments had better control effects on silicate and silica than the two EMF treatments. Compared with EMF, PMF decreased the content silicate and silica by 10.2-33.3% and 8.5-29.2%, respectively. In addition, the intensity in PMF groups and the frequency in EMF groups had impacts on the silica fouling content. PMF_900mT reduced the content of silicate and silica by 10.4-12.5% and 11.8-14.3% compared with PMF_600mT, while EMF_20 kHz decreased the content of silicate and silica by 14.1-15.4% and 7.4-9.2% compared with EMF_30 kHz.

Variations of unit-cell parameters of silicate and silica particulate fouling are shown in Fig. 5c, 5f, and 5i. The results show that the MF had slight effect on the unit-cell parameters of the three types of silicates and silica. Compared with the CK, MF treatments increased the unit cell volume of chlorites, muscovite, anorthite and silica by 0.2-2.2Å^3. The increase in the bond lengths of Mg-Al, Al-O, Si-Ca and Ca-O among the three silicate components and silica was similarly small, since only were increased by 0.001%-0.005%.

#Fig. 5 approximately here#

3.5 Influence path of MF on fouling

Obvious correlations were found between the contents of various minerals and water quality. For instance, significant ($p < 0.05$) interactions were found between calcium carbonate and silica fouling (Fig.

229   6a,). SEMA (Fig. 6b) was further applied to reveal the direct-indirect effects on MF on fouling. MF

230   presented significant ($p < 0.05$) negative correlations with calcium carbonate and silica fouling, and the

231   absolute standardized path coefficient was 0.89 and 0.71, respectively. Compared with silica fouling, MF

232   illustrated stronger effect on calcium carbonate fouling. Furthermore, silica fouling and calcium

233   carbonate fouling have strong effects on fouling dry weight. SEMA also showed that there were obvious

234   synergistic interactions between calcium carbonate and silica fouling, being the correlation coefficients

235   was 0.72. Thus, SEMA results suggested that, on one hand, MF could directly reduce the contents of

236   silica fouling and calcium carbonate fouling. On the other hand, MF indirectly controlled the silica

237   fouling by reducing the calcium carbonate fouling.

238   #Fig. 6 approximately here#

4 Discussion

4.1 Inhibition mechanism of MFs on calcium - silica fouling

241   Previous studies demonstrated the MF has significant inhibition effects on calcium carbonate

242   fouling (Al Helal et al. 2019, Alimi et al. 2009), this study also found that MF decreased the carbonate

243   contents in BWDS. One possible reason is that MF has been proved to be able to weaken the hydrogen

244   bond force between water molecules. Thus, MF can decompose water clusters into monomers or small

245   clusters, resulting in the reduction of water surface tension (Fig. 3). The changes in water clusters can

246   increase the collision chance between Ca^{2+} and HCO_3^-, and shorten the crystallization induction period,

247   leading to accelerated formation of hydrated amorphous $CaCO_3$ (Han et al. 2018). In addition, MF could

248   increase the Gibbs free energy of crystals (Tai et al. 2011), which further trigger the transformation of

249    $CaCO_3$ crystal form from calcite to aragonite. The aragonite has looser structure than calcite, and could

250   be easily flushed out with the water flow from pipeline surfaces (Li et al. 2019). In other words, MF

251   reduced the carbonates content by changing the crystal form of carbonates. On other hand, this study

252   found the crystal structures of carbonate were changed after the MF application. The minerals have tiny

253   crystal cells. The physical properties of minerals, such as porosity and hardness, are closely related to the

254   structural parameters of cell (Glasser and Jenkins 2000). This study found the MF increased the cell

255   volumes of calcite and aragonite. The increase in cell volume would consequently decrease specific

256   surface area of crystals (Cordeiro et al. 2011), and reduction in the adsorption energy of the crystals,

257   making the carbonates easily to be flushed out with flow. In addition, MF increased the bond length of

258   carbonates, such as Ca-Ca and Ca-C, which will reduce the strength of chemical bonds (Jenkins et al.

259   1999). The increase in bond length also leads to the reduction of crystal hardness (Simunek and Vackar

260   2006), and avoids forming hard fouling structures. Consequently, due to the brittleness of crystal was

261   increased, crystal was easily to be broken by the water shear stresses, thus prevented the precipitations

262   fouling formation.

263   Silica and silicate particulates both are most abundant in brackish surface waters, transported

264   through the BWDS networks and accumulates at the bottom of the pipelines (Deponte et al. 2019, Zhang

265   et al. 2017a). In addition, brackish water contains high concentration of silica (Subramani et al. 2012)

266   which is consistent with the results in this paper (Fig. 7). Thus, due to chemical reaction it becomes easy

267   to form silica fouling on pipeline (German et al. 2019). Moreover, silica fouling is difficult to remove

268   because it is hard and insoluble in common acid and alkali (Euvrard et al. 2007, Sasan et al. 2017).

269   However, this study found the MF application effectively reduces the contents of silicate and silica in

270   BWDS (Fig 5). This might be due to MF compresses the electric double layer of colloidal particles

271   (Koshoridze and Levin 2014), resulting in the reduction of absolute value of zeta potential on the surface

272   of silica and silicates (Fig.7 c). The relatively low absolute value of zeta potential indicates that the

273 adsorption capacity between silica and silicate particles was enhanced, leading to flocculation between

274 particles (Pinto and Buss 2020). Therefore, MF increases the particle size in BW by flocculation (Fig.7a).

275 Before entering the BWDS, such flocs with large size were easy to be settled down on the surface of

276 pipelines and filtered by the screen filter, which would avoid the depositions of silicates and silica in

277 BWDS. It is found that combined use of MF and screen filter can reduce the suspended particles in BW

278 by 19.4-30.6%, compared with CK using only screen filters (Fig. 7d).

279 **4.2 Interactions between silica- calcium carbonate fouling in MF**

280   High concentration of total dissolved salts, and suspended silica solids involved in BW (Mahmoudi

281 et al. 2010, Thuy et al. 2007), composite calcium – silica fouling was a persistent problem in BWDS

282 (German et al. 2019, Lee et al. 2020). However, due to the constraints of experimental conditions, most

283 researchers use the synthetic water instead of brackish water to carry out indoor simulation experiments

284 to explore the effect of MF on fouling (Alimi et al. 2009, Rouina et al. 2016). There are huge differences

285 between the synthetic and brackish water, and single $CaCO_3$ fouling is often formed in synthetic water.

286 Previous reports have shown that, due to the interaction between composite fouling (Fig. 6a) became

287 more difficult to remove than single fouling (Zhou et al. 2019) . Therefore, we collected the literature

288 about the effect of MF on calcium carbonate under the water distribution, and compared the scale

289 inhibition rate in the literature with our results.

290   This study found that MF decreased the carbonate inhibition content by 60.7%, which was higher

291 than the inhibition rates (4%-46.7%) reported by previous studies (Chibowski et al. 2003, Sohaili et al.

292 2016, Tijing et al. 2011). This might be because of the interactions between silica- calcium carbonate

293 fouling was broken with MF treatment. With MF application, the thickness of hydration film on the

294 surfaces of the silicates and silica were reduced, which may increase the adsorption capacity of silica

14

295   particles to cations (e.g. Ca^{2+}), reduce the concentration of water cations (Szkatula et al. 2002), and

296   caused the carbonate precipitation were hard to be formed in BWDS. In addition, previous reports have

297   shown that silica solution may promote the formation of amorphous calcium carbonate when pH value

298   was high in water (Kellermeier et al. 2012) . Our results illustrated that MF could increase the pH value

299   (Fig 2), which indirectly affected the formation of $CaCO_3$ fouling. On the contrary, carbonate can serve

300   as the nucleation sites for the formation of silicate (Umar et al. 2013). Once carbonates are formed, it is

301   easy for silicate to deposit on the surface of carbonates (Schilde et al. 2013). Since MF effectively

302   controlled the carbonate precipitations, MF may indirectly lead to the reductions in silicate contents. In

303   addition, MF also promoted the polymerization of calcium and magnesium ions with soluble silicon in

304   BW, resulting in the reduction of soluble silica content in BW (Fig. 7b) , and the increase of silicate

305   precipitation, which settled before entering BWDS. Moreover, MF promoted the crystal form of

306   carbonate from calcite to aragonite. Shen et al. (2019) study have demonstrated that the aragonite has

307   less adhesion to silicates and silica in comparison with calcite, which may also lead to the reductions of

308   silicates and silica in MF-treated groups.

309   **4.3 MF device selection and engineering application**

310   Although the results proved that MF effectively controlled the composite fouling in BWDS, it is

311   necessary to evaluate the engineering implications of the results for the successful application of MF (Fig

312   S2). Acidification, the most common method for mitigating fouling in agricultural BWDS, was compared

313   with MF. Our results show that anti-fouling ability of acid treatment was slightly better 0.77-8.44% than

314   MF (Aali et al. 2009). However, the scale inhibition effect of acid treatment could not be maintained in

315   long term. Frequent acid flushing is required to maintain the fouling inhibition. On the other hand, due

316   to the stable physiochemical properties of silicates and silica, the acidification does not always perform

317 better. While MF could control the deposition of silicates and silica, which is more powerful in

318 controlling silica fouling. As for environmental risks, acid injection would frequently contribute to soil

319 acidification, soil hardness and, consequently, cause damages to crop growth (Jozefaciuk et al. 2000,

320 Song et al. 2019). However, the environmental risks associated with MF is mainly due to the electricity

321 consumption by EMF, therefore MF could be considered as a cleaner, and more environmentally friendly

322 fouling inhibition method. In addition, MF has been proved to be able to improve soil structure and

323 enhance crop yields (Hachicha et al. 2018). Capital costs is another major factor closely related with the

324 successful implications of anti-fouling methods. In comparison, the initial costs of MF are lower, and no

325 additional operating costs are needed. Thus, the accumulative costs of permanent magnetic field during

326 the 1000 h is only \$245.3, while during the same operating hours, acid treatments would need acid

327 injection for a couple of times, which would further increase the labor cost. The total cost of technology

328 reached \$703.3 shown in supplementary material, section 3. Therefore, the operating cost of MF during

329 is much lower than the acidification. Based on these results, the MF is a promising method of fouling

330 control in agricultural BWDS.

331   This study also observed that the anti-fouling efficiency among different MF types varied greatly.

332 The fouling mitigation ability of PMF was higher than EMF. The better anti-fouling ability in PMF

333 treatments are attributed to the different responses of water quality with the two types of MF generation

334 methods. It was observed that the water quality parameters in PMF treatments were changed more greatly

335 than EMF treatments (Fig. 2). This was probably due to the magnetic flux density of MF in PMF

336 treatments were higher than EMF treatments. The MF magnetic flux density in PMF treatments ranged

337 600 - 900 mT, while the magnetic flux density were less than 300 Gs in EMF treatments. Chang and Tai

338 (2010) found that the higher of MF magnetic flux density, the higher fouling inhibition efficiency.

Meanwhile, the cost of the PMF magnetizer is only about 20% of the EMF magnetizer, and there is no external consumption of electricity in PMF treatments. Therefore, PMF is highly recommended for composite fouling inhibition in BWDS. Moreover, in this study, efficiency of fouling removal is further enhanced by 13.6-15.2% using a higher magnetic strength of 900mT. Some scholars have also found the stronger magnetic field (400mT–1500mT) the application of PMF promotes the precipitation of aragonite polymorph of $CaCO_3$ (Knez and Pohar 2005, Kobe et al. 2002). At high magnetic strength, plausibly the fouling have greater ionic charge and more energy for the charged particles to vibrate. However, there should be an amenable range of magnetic strength to be installed in the treatment device and it is recommended to be between 900m T and 1500m T.

5 Conclusions

(1) MF (magnetic field) significantly inhibited the formation of composite calcium -silica fouling in brackish water distribution systems, and the fouling inhibition rate reached 30.2-54.8%. Moreover, MF effectively alleviated the clogging of brackish water distribution systems, and increased the Dra by 26.5-49.7%;

(2) MF reduced the calcite content by 38.2%-64.3% and increased the aragonite content by 15.5-48.8%. In addition, MF increased the unit cell volume (Cv) of calcite and aragonite by 11.4-43.43 $Å^3$ and 7.2-31.73 $Å^3$, and the Ca-Ca and Ca-C bonds of calcite increased by 0.1-0.5% and 0.3-1.5%, the Ca-Ca and Ca-C bonds of aragonite increased by 0.1-0.4% and 0.3-1.1%. Finally, MF decreased the calcium carbonate fouling content by 33.4-60.7%.

(3) MF reduced the content of three types of silicates (chlorites, muscovite and anorthite) by 0.97-2.44 mg cm^{-2}, 0.53-1.06 mg cm^{-2}, 0.75-1.45 mg cm^{-2}, respectively, and finally reduced the accumulative content of silicate by 21.8-47.9%, and silica reduced by 22.7%-44.3%.

(4) Different MF treatment will significantly affect the formation of composite calcium carbonate -

silica fouling. Compared with EMF, the fouling inhibition rate of PMF increased by 12.3-35.1%. And

PMF 900 mT was 13.6-15.2% higher than PMF 600 mT, while, EMF 20 kHz was 10.9-12.6% higher

than EMF 30 kHz. This study recommends using PMF 900 mT to control composite calcium -silica

fouling

Acknowledgements

References

Aali, K.A., Liaghat, A. and Dehghanisanij, H. (2009) The effect of acidification and magnetic field on emitter

clogging under saline water application. Journal of Agricultural Science (Toronto) 1(1), 132-141.

Al-Sabagh, A.M., El Basiony, N.M., Sadeek, S.A. and Migahed, M.A. (2018) Scale and corrosion inhibition

performance of the newly synthesized anionic surfactant in desalination plants: Experimental, and theoretical

investigations. Desalination 437, 45-58.

Al Helal, A., Soames, A., Iglauer, S., Gubner, R. and Barifcani, A. (2019) The influence of magnetic fields on

calcium carbonate scale formation within monoethylene glycol solutions at regeneration conditions. Journal

of Petroleum Science and Engineering 173, 158-169.

Aliaskari, M. and Schafer, A.I. (2021) Nitrate, arsenic and fluoride removal by electrodialysis from brackish

groundwater. Water Research 190, 116683-116683.

Alimi, F., Tlili, M., Ben Amor, M., Maurin, G. and Gabrielli, C. (2009) Influence of magnetic field on calcium

carbonate precipitation in the presence of foreign ions. Surface Engineering and Applied Electrochemistry

45(1), 56-62.

384 Antony, A., Subhi, N., Henderson, R.K., Khan, S.J., Stuetz, R.M., Le-Clech, P., Chen, V. and Leslie, G. (2012)

385 Comparison of reverse osmosis membrane fouling profiles from Australian water recycling plants. Journal of

386 Membrane Science 407, 8-16.

387 Chang, M.C. and Tai, C.Y. (2010) Effect of the magnetic field on the growth rate of aragonite and the

388 precipitation of CaCO3. Chemical Engineering Journal 164(1), 1-9.

389 Chang, Y.S., Ooi, B.S., Ahmad, A.L., Leo, C.P. and Low, S.C. (2021) Vacuum membrane distillation for

390 desalination: Scaling phenomena of brackish water at elevated temperature. Separation and Purification

391 Technology 254.

392 Chibowski, E., Holysz, L. and Szczes, A. (2003) Adhesion of in situ precipitated calcium carbonate in the

393 presence and absence of magnetic field in quiescent conditions on different solid surfaces. Water Research

394 37(19), 4685-4692.

395 Cordeiro, G.C., Toledo Filho, R.D., Tavares, L.M., Rego Fairbairn, E.d.M. and Hempel, S. (2011) Influence

396 of particle size and specific surface area on the pozzolanic activity of residual rice husk ash. Cement &

397 Concrete Composites 33(5), 529-534.

398 Demadis, K.D., Neofotistou, E., Mavredaki, E., Tsiknakis, M., Sarigiannidou, E.M. and Katarachia, S.D. (2005)

399 Inorganic foulants in membrane systems: chemical control strategies and the contribution of "green chemistry".

400 Desalination 179(1-3), 281-295.

401 Deponte, H., Rohwer, L., Augustin, W. and Scholl, S. (2019) Investigation of deposition and self-cleaning

402 mechanism during particulate fouling on dimpled surfaces. Heat and Mass Transfer 55(12), 3633-3644.

403 Du, J.R., Zhang, X., Feng, X., Wu, Y., Cheng, F. and Ali, M.E.A. (2020) Desalination of high salinity brackish

404 water by an NF-RO hybrid system. Desalination 491.

405 Euvrard, M., Hadi, L. and Foissy, A. (2007) Influence of PPCA (phosphinopolycarboxylic acid) and DETPMP

(diethylenetriaminepentamethylenephosphonic acid) on silica fouling. Desalination 205(1-3), 114-123.

Fathi, A., Mohamed, T., Claude, G., Maurin, G. and Mohamed, B.A. (2006) Effect of a magnetic water treatment on homogeneous and heterogeneous precipitation of calcium carbonate. Water Research 40(10), 1941-1950.

Florez, M., Martinez, E. and Victoria Carbonell, M. (2012) Effect of Magnetic Field Treatment on Germination of Medicinal Plants Salvia officinalis L. and Calendula officinalis L. Polish Journal of Environmental Studies 21(1), 57-63.

Garcia, S. and Trueba, A. (2018) Influence of the Reynolds number on the thermal effectiveness of tubular heat exchanger subjected to electromagnetic field-based antifouling treatment in an open once-through seawater cooling system. Applied Thermal Engineering 140, 531-541.

German, M.S., Dong, H., Schevets, A., Smith, R.C. and SenGupta, A.K. (2019) Field validation of self-regenerating reversible ion exchange-membrane (RIX-M) process to prevent sulfate and silica fouling. Desalination 469.

Glasser, L. and Jenkins, H.D.B. (2000) Lattice energies and unit cell volumes of complex ionic solids. Journal of the American Chemical Society 122(4), 632-638.

Greenlee, L.F., Lawler, D.F., Freeman, B.D., Marrot, B. and Moulin, P. (2009) Reverse osmosis desalination: Water sources, technology, and today's challenges. Water Research 43(9), 2317-2348.

Guo, H., Hu, Z., Zhang, H., Hou, Z. and Min, W. (2019) Soil Microbial Metabolic Activity and Community Structure in Drip-Irrigated Calcareous Soil as Affected by Irrigation Water Salinity. Water Air and Soil Pollution 230(2).

Hachicha, M., Kahlaoui, B., Khamassi, N., Misle, E. and Jouzdan, O. (2018) Effect of electromagnetic treatment of saline water on soil and crops. Journal of the Saudi Society of Agricultural Sciences 17(2), 154-

428   162.

429   Han, Y., Zhang, C.X., Wu, L.C., Zhang, Q.R., Zhu, L. and Zhao, R.K. (2018) Influence of alternating

430   electromagnetic field and ultrasonic on calcium carbonate crystallization in the presence of magnesium ions.

431   Journal of Crystal Growth 499, 67-76.

432   Hanikel, N., Prevot, M.S. and Yaghi, O.M. (2020) MOF water harvesters. Nature Nanotechnology 15(5), 348-

433   355.

434   Holysz, L., Chibowski, E. and Szczes, A. (2003) Influence of impurity ions and magnetic field on the

435   properties of freshly precipitated calcium carbonate. Water Research 37(14), 3351-3360.

436   Jenkins, H.D.B., Roobottom, H.K., Passmore, J. and Glasser, L. (1999) Relationships among ionic lattice

437   energies, molecular (formula unit) volumes, and thermochemical radii. Inorganic Chemistry 38(16), 3609-

438   3620.

439   Johan, S., Shi, H., Lavania, B., Noorul Hassan, Z., Noraziah, A. and Shantha Kumari, M. (2016) Removal of

440   scale deposition on pipe walls by using magnetic field treatment and the effects of magnetic strength. Journal

441   of Cleaner Production 139, 1393-1399.

442   Jozefaciuk, G., Hoffmann, C., Renger, M. and Marschner, B. (2000) Effect of extreme acid and alkali treatment

443   on surface properties of soils. Journal of Plant Nutrition and Soil Science 163(6), 595-601.

444   Kellermeier, M., Gebauer, D., Melero-Garcia, E., Drechsler, M., Talmon, Y., Kienle, L., Coelfen, H., Manuel

445   Garcia-Ruiz, J. and Kunz, W. (2012) Colloidal Stabilization of Calcium Carbonate Prenucleation Clusters with

446   Silica. Advanced Functional Materials 22(20), 4301-4311.

447   Knez, S. and Pohar, C. (2005) The magnetic field influence on the polymorph composition of CaCO3

448   precipitated from carbonized aqueous solutions. Journal of Colloid and Interface Science 281(2), 377-388.

449   Kobe, S., Drazic, G., Cefalas, A.C., Sarantopoulou, E. and Strazisar, J. (2002) Nucleation and crystallization

450   of CaCO3 in applied magnetic fields. Crystal Engineering 5(3-4), 243-253.

451   Koshoridze, S.I. and Levin, Y.K. (2014) The influence of a magnetic field on the coagulation of nanosized

452   colloid particles. Technical Physics Letters 40(8), 716-719.

453   Lee, W.J., Ng, Z.C., Hubadillah, S.K., Goh, P.S., Lau, W.J., Othman, M.H.D., Ismail, A.F. and Hilal, N. (2020)

454   Fouling mitigation in forward osmosis and membrane distillation for desalination. Desalination 480.

455   Li, L., Cao, M. and Yin, H. (2019) Comparative roles between aragonite and calcite calcium carbonate

456   whiskers in the hydration and strength of cement paste. Cement & Concrete Composites 104.

457   Ma, C., Xiao, Y., Puig-Bargues, J., Shukla, M.K., Tang, X., Hou, P. and Li, Y. (2020) Using phosphate fertilizer

458   to reduce emitter clogging of drip fertigation systems with high salinity water. Journal of Environmental

459   Management 263.

460   Mahmoudi, H., Spahis, N., Goosen, M.F., Ghaffour, N., Drouiche, N. and Ouagued, A. (2010) Application of

461   geothermal energy for heating and fresh water production in a brackish water greenhouse desalination unit: A

462   case study from Algeria. Renewable & Sustainable Energy Reviews 14(1), 512-517.

463   Muhammad, T., Zhou, B., Liu, Z., Chen, X. and Li, Y. (2021) Effects of phosphorus-fertigation on emitter

464   clogging in drip irrigation system with saline water. Agricultural Water Management 243.

465   Nthunya, L.N., Gutierrez, L., Lapeire, L., Verbeken, K., Zaouri, N., Nxumalo, E.N., Mamba, B.B., Verliefde,

466   A.R. and Mhlanga, S.D. (2019) Fouling-resistant PVDF nanofibre membranes for the desalination of brackish

467   water in membrane distillation. Separation and Purification Technology 228.

468   Park, S., Nam, T., You, J., Eun-Sik, K., Choi, I., Park, J. and Cho, K.H. (2019) Evaluating membrane fouling

469   potentials of dissolved organic matter in brackish water. Water Research 149, 65-73.

470   Pinto, I. and Buss, A. (2020) zeta Potential as a Measure of Asphalt Emulsion Stability. Energy & Fuels 34(2),

471   2143-2151.

472 Rouina, M., Kariminia, H.-R., Mousavi, S.A. and Shahryari, E. (2016) Effect of electromagnetic field on

473 membrane fouling in reverse osmosis process. Desalination 395, 41-45.

474 Sasan, K., Brady, P.V., Krumhansl, J.L. and Nenoff, T.M. (2017) Removal of dissolved silica from industrial

475 waters using inorganic ion exchangers. Journal of Water Process Engineering 17, 117-123.

476 Schilde, C., Hanisch, C., Naumann, D., Beierle, T. and Kwade, A. (2013) A novel way to vary the structure of

477 precipitated silica and calcium carbonate aggregates in a wide range by using grinding media during the

478 precipitation process. Chemical Engineering Science 94, 127-137.

479 Shemer, H., Melki-Dabush, N. and Semiat, R. (2019) Removal of silica from brackish water by integrated

480 adsorption/ultrafiltration process. Environmental Science and Pollution Research 26(31), 31623-31631.

481 Shen, C., Wang, Y., Tang, Z., Yao, Y., Huang, Y. and Wang, X. (2019) Experimental study on the interaction

482 between particulate fouling and precipitation fouling in the fouling process on heat transfer tubes. International

483 Journal of Heat and Mass Transfer 138, 1238-1250.

484 Simunek, A. and Vackar, J. (2006) Hardness of covalent and ionic crystals: First-principle calculations.

485 Physical Review Letters 96(8).

486 Sohaili, J., Shi, H.S., Lavania, B., Zardari, N.H., Ahmad, N. and Muniyandi, S.K. (2016) Removal of scale

487 deposition on pipe walls by using magnetic field treatment and the effects of magnetic strength. Journal of

488 Cleaner Production 139, 1393-1399.

489 Song, P., Feng, G., Brooks, J., Zhou, B., Zhou, H., Zhao, Z. and Li, Y. (2019) Environmental risk of chlorine-

490 controlled clogging in drip irrigation system using reclaimed water: the perspective of soil health. Journal of

491 Cleaner Production 232, 1452-1464.

492 Sriramulu, D., Vafakhah, S. and Yang, H.Y. (2019) Activated Luffa derived biowaste carbon for enhanced

493 desalination performance in brackish water. Rsc Advances 9(26), 14884-14892.

494   Subramani, A., DeCarolis, J., Pearce, W. and Jacangelo, J.G. (2012) Vibratory shear enhanced process (VSEP)

495   for treating brackish water reverse osmosis concentrate with high silica content. Desalination 291, 15-22.

496   Suharso, Buhani, Utari, H.R., Tugiyono and Satria, H. (2019) Influence of gambier extract modification as

497   inhibitor of calcium sulfate scale formation. Desalination and Water Treatment 169, 22-28.

498   Szkatula, A., Balanda, M. and Kopec, M. (2002) Magnetic treatment of industrial water. Silica activation.

499   European Physical Journal-Applied Physics 18(1), 41-49.

500   Tai, C.Y., Chang, M.C. and Yeh, S.W. (2011) Synergetic effects of temperature and magnetic field on the

501   aragonite and calcite growth. Chemical Engineering Science 66(6), 1246-1253.

502   Thuy, T., Bolto, B., Gray, S., Manh, H. and Ostarcevic, E. (2007) An autopsy study of a fouled reverse osmosis

503   membrane element used in a brackish water treatment plant. Water Research (Oxford) 41(17), 3915-3923.

504   Tijing, L.D., Lee, D.-H., Kim, D.-W., Cho, Y.I. and Kim, C.S. (2011) Effect of high-frequency electric fields

505   on calcium carbonate scaling. Desalination 279(1-3), 47-53.

506   Trueba, A., Garcia, S., Otero, F.M., Vega, L.M. and Madariaga, E. (2015) The effect of electromagnetic fields

507   on biofouling in a heat exchange system using seawater. Biofouling 31(1), 19-26.

508   Umar, A.A., Saaid, I.B.M.J.R.J.o.A.S.E. and Technology (2013) Silicate Scales Formation During ASP

509   Flooding: A Review. 6(9), 1543-1555.

510   Urusovskaya, A.A., Alshits, V.I., Smirnov, A.E. and Bekkauer, N.N. (2003) The influence of magnetic effects

511   on the mechanical properties and real structure of nonmagnetic crystals. Crystallography Reports 48(5), 796-

512   812.

513   Wang, S., Huang, X. and Elimelech, M. (2020) Complexation between dissolved silica and alginate molecules:

514   Implications for reverse osmosis membrane fouling. Journal of Membrane Science 605.

515   Wang, Y., Babchin, A.J., Chernyi, L.T., Chow, R.S. and Sawatzky, R.P. (1997) Rapid onset of calcium

516   carbonate crystallization under the influence of a magnetic field. Water Research 31(2), 346-350.

517   Xiao, Y., Seo, Y., Lin, Y., Li, L., Muhammad, T., Ma, C. and Li, Y. (2020) y Electromagnetic fields for

518   biofouling mitigation in reclaimed water distribution systems. Water Research 173.

519   Zhang, L., Hu, B., Song, H., Yang, L. and Ba, L. (2017a) Colloidal Force Study of Particle Fouling on Gas

520   Capture Membrane. Scientific Reports 7.

521   Zhang, L., Huang, R., Tao, P., Song, C., Wu, J., Deng, T. and Shang, W. (2017b) Occlusion of magnetic

522   nanoparticles within calcium carbonate single crystals under external magnetic field. Pure and Applied

523   Chemistry 89(12), 1741-1750.

524   Zhang, Y., Li, X., Simunek, J., Shi, H., Chen, N., Hu, Q. and Tian, T. (2021) Evaluating soil salt dynamics in

525   a field drip-irrigated with brackish water and leached with freshwater during different crop growth stages.

526   Agricultural Water Management 244.

527   Zhou, H., Li, Y., Wang, Y., Zhou, B. and Bhattarai, R. (2019) Composite fouling of drip emitters applying

528   surface water with high sand concentration: Dynamic variation and formation mechanism. Agricultural Water

529   Management 215, 25-43.

530

Captions for Figures and Tables in the Paper

Fig. 1 Layout of the test system platform.

Fig. 2. Effects of MF on water quality, fouling content and BWDS performance.

Fig. 3. Effect of MF on proportions of mineral components and fouling surface morphology

Fig. 4. Variations of content and unit-cell parameters of calcium carbonate fouling

Fig. 5. Variations of content and unit-cell parameters of silica fouling

Fig. 6. Correlation among BWDS performance, mineral components and water quality

Fig. 7. Effects of MF on suspended matter, silica concentration and particle size

Table. 1. Water quality characteristics tested during the experiment
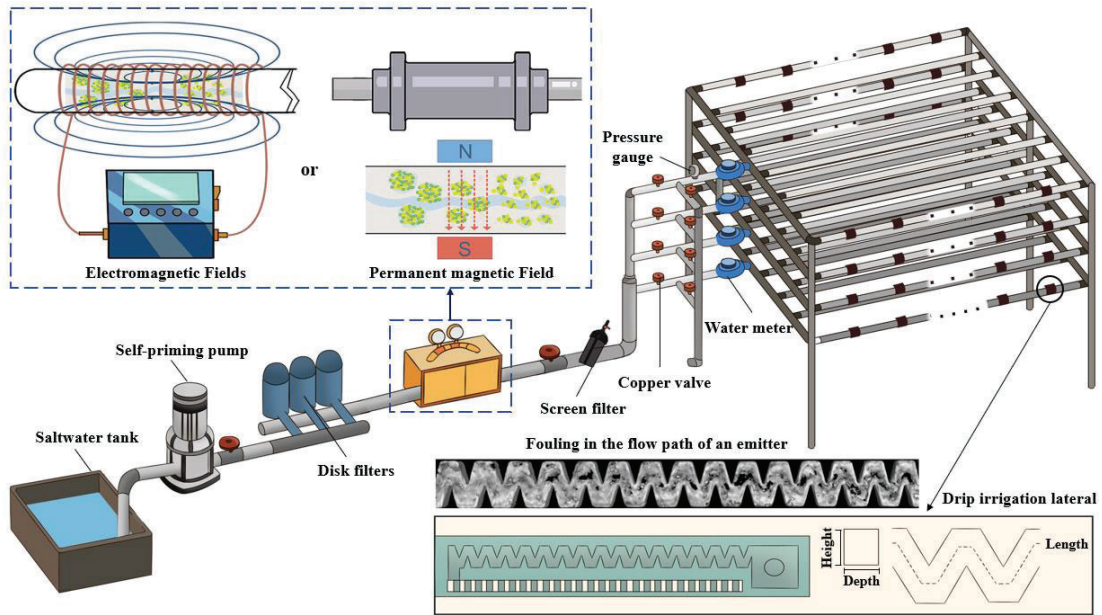
Fig. 1. Layout of the test system platform

Note: taking EMFs and PMF treatments as an example, the non-MF groups did not contain magnetizers.
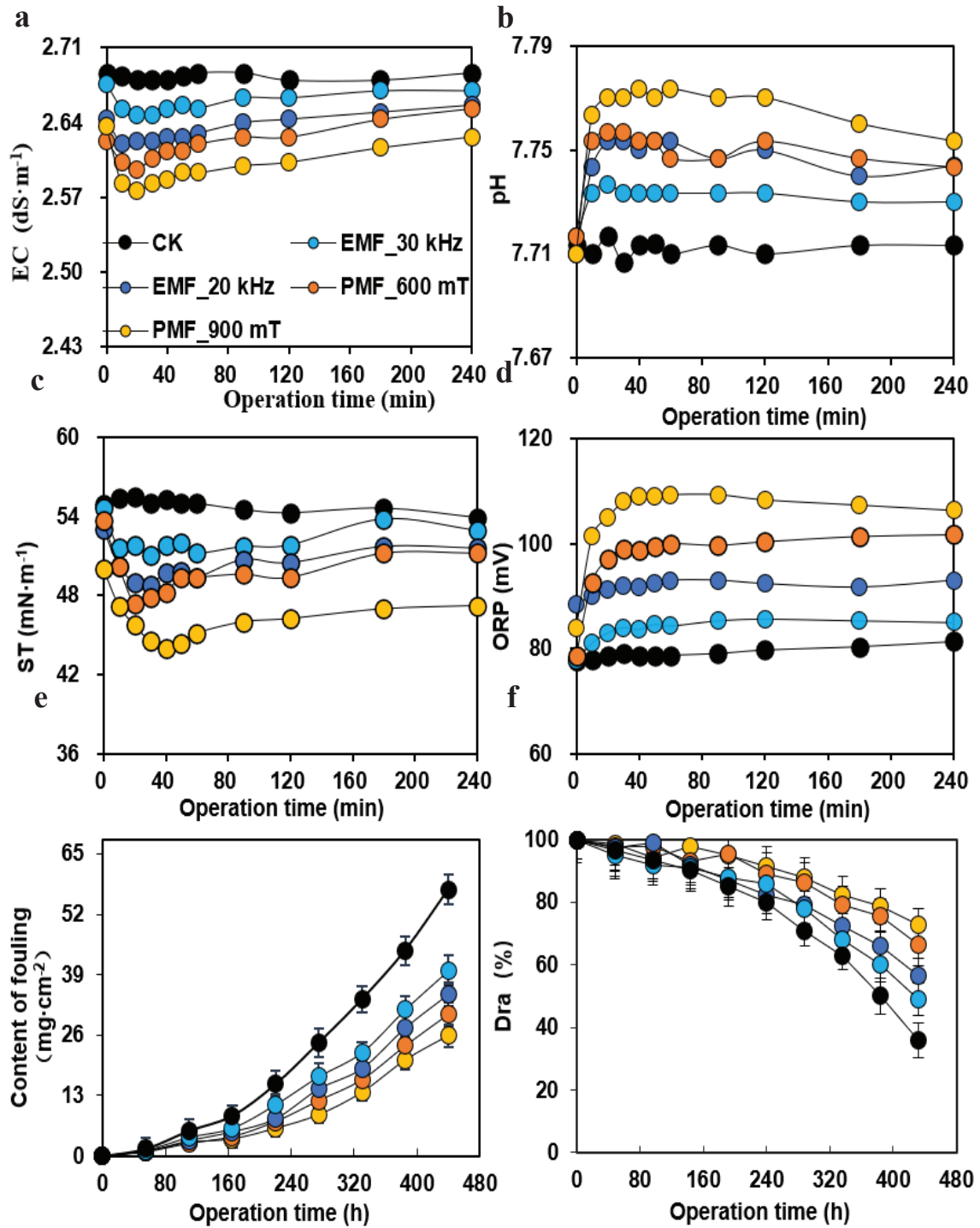
Fig. 2 Effects of MF on water quality, fouling content and BWDS performance.

(a) EC, Electrical conductivity; (b) pH, Potential of hydrogen; (c) ST, Surface Tension; (d) ORP, Oxidation-Reduction

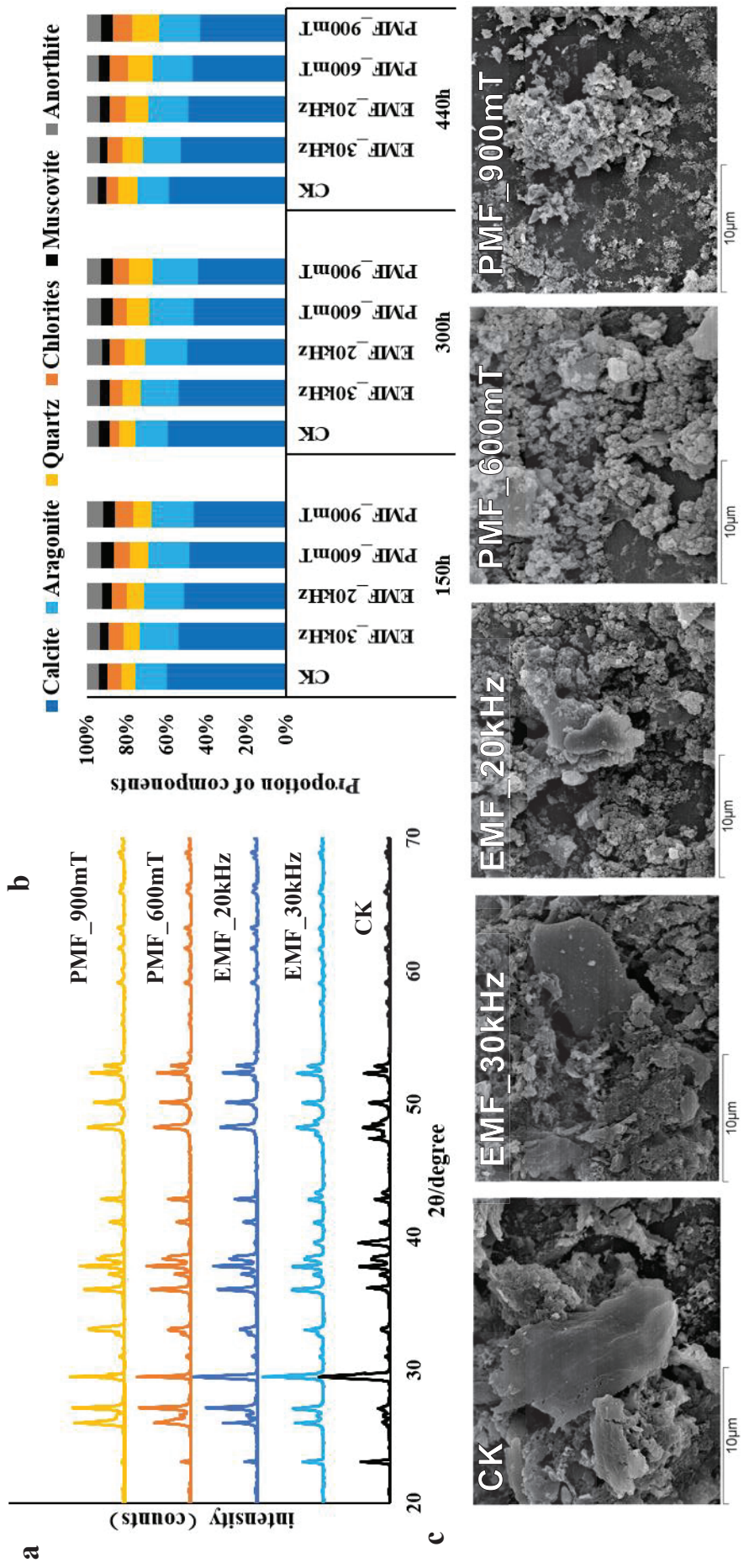Potential; (e) Content of Fouling; (f) BWDS performances, average discharge variation rate (Dra) of BWDS

Fig. 3. The influence of MF on the mineral component proportions and appearance of fouling

Note: (a) represent the XRD diffraction pattern, (b) represent the proportion of mineral components under MF, (c) represent the surface morphology of fouling treated by CK, EMF_30kHz, EMF_20kHz, PMF_600mT, PMF_900mT
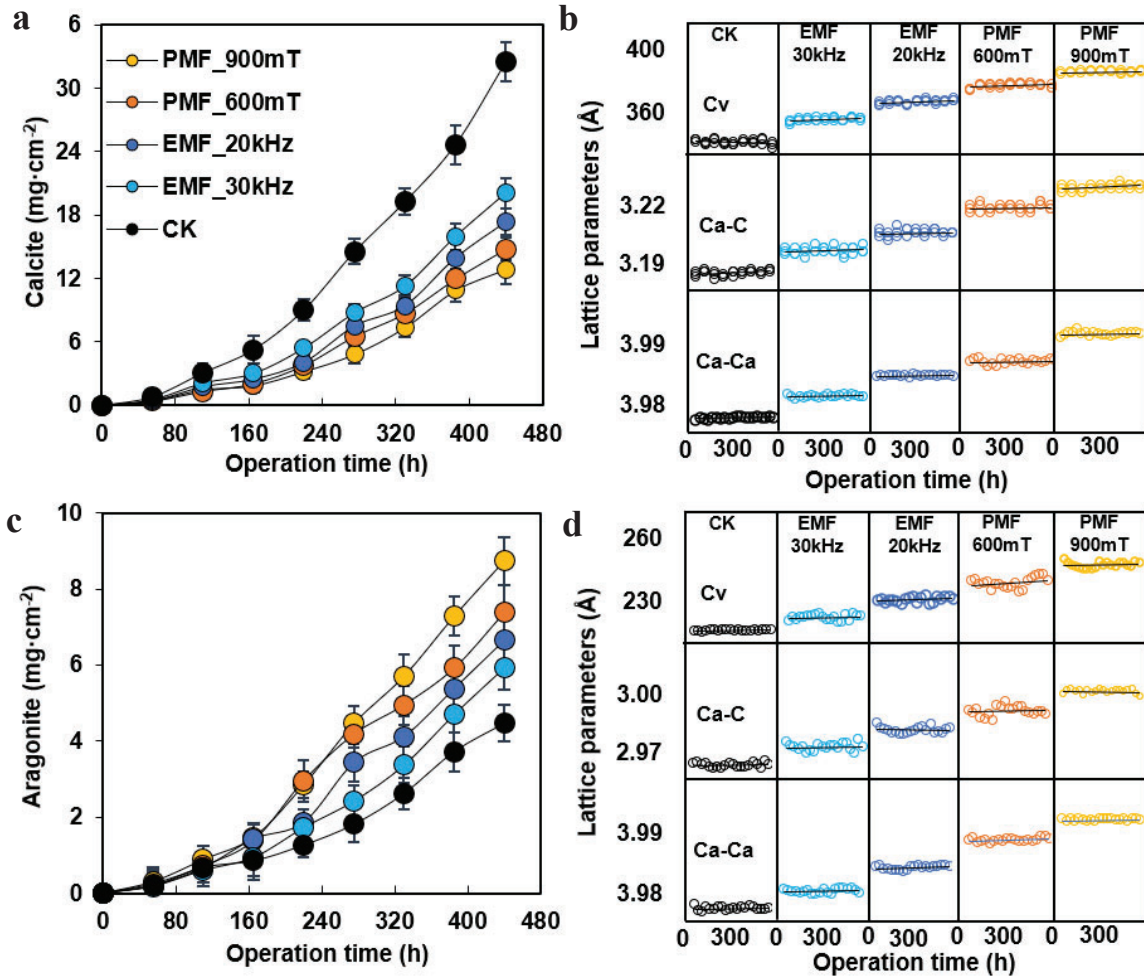
Fig. 4. Variation of content and unit-cell parameters of calcium carbonate fouling.

(a) content of calcite; (c) content of aragonite; (b) and (d) the unit-cell parameters of calcite and aragonite. Cv is cell volume of mineral, Ca-C and Ca-Ca are bond length etc.
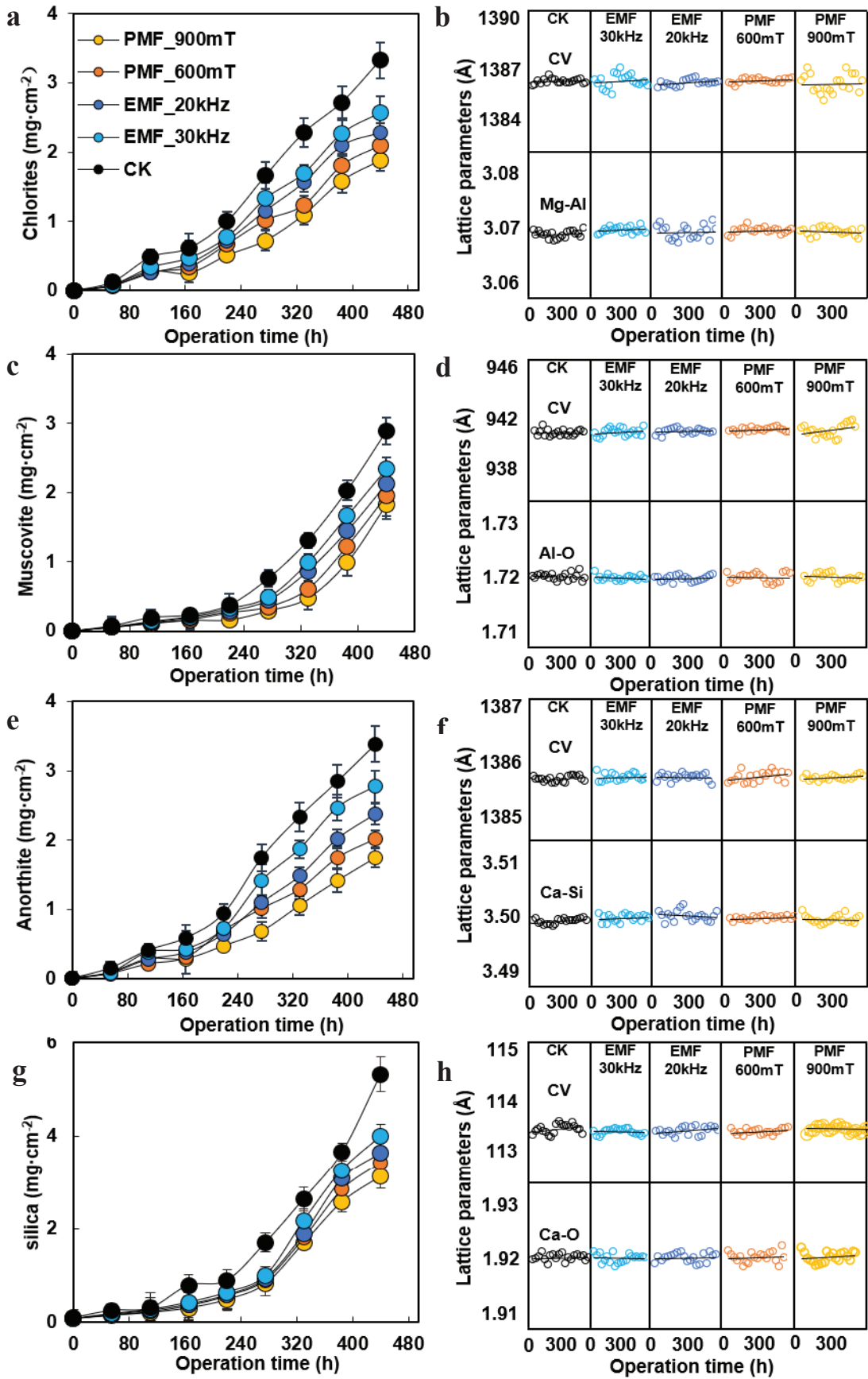
Fig. 5. Variation of content and unit-cell parameters of silica fouling

(a)   chlorites, (c) muscovite, (e) anorthite, and (g) silica; and their unit-cell parameters (b), (d), (f), and (h)
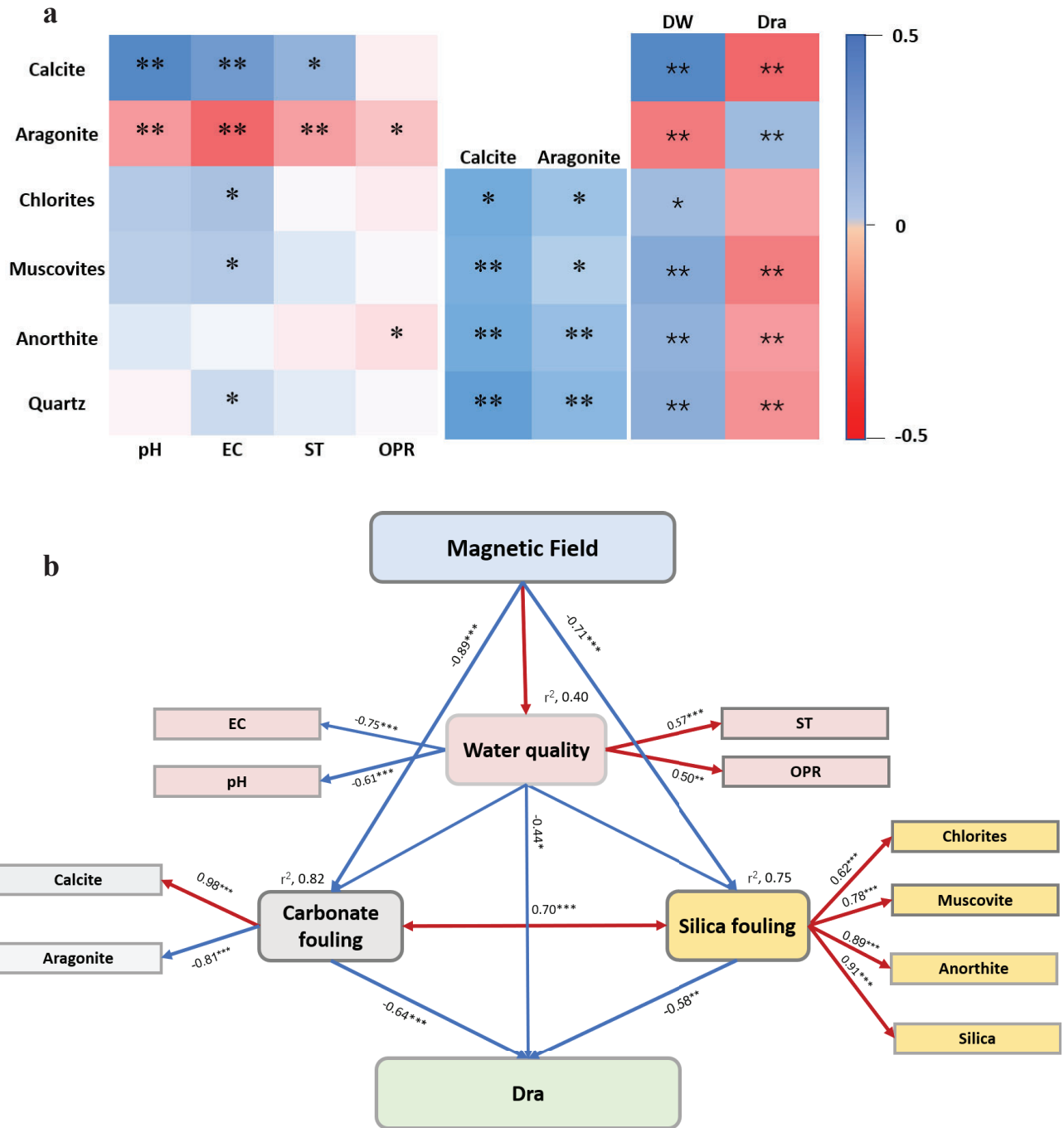
31

Fig. 6. Correlation between BSWDS performance, mineral components and water quality parameters

Note: (a) Spearman correlation of water quality, minerals, Dra and DW; (b) is the structural equation model analysis (SEMA). The SEMA shows the relationship between the MF treatment, the content of the mineral component and the water quality. Red and blue radial lines respectively represented significant positive correlation (p<0.05) and significant negative correlation (p<0.05). The red double-headed arrows represent positive and negative interactions, respectively, and the thickness of the arrow represents the strength of the correlation. The number on the arrow represents the standard path coefficient (β). Model testing parameters (χ^2=18.3, df=7, n=1294 independent samples).
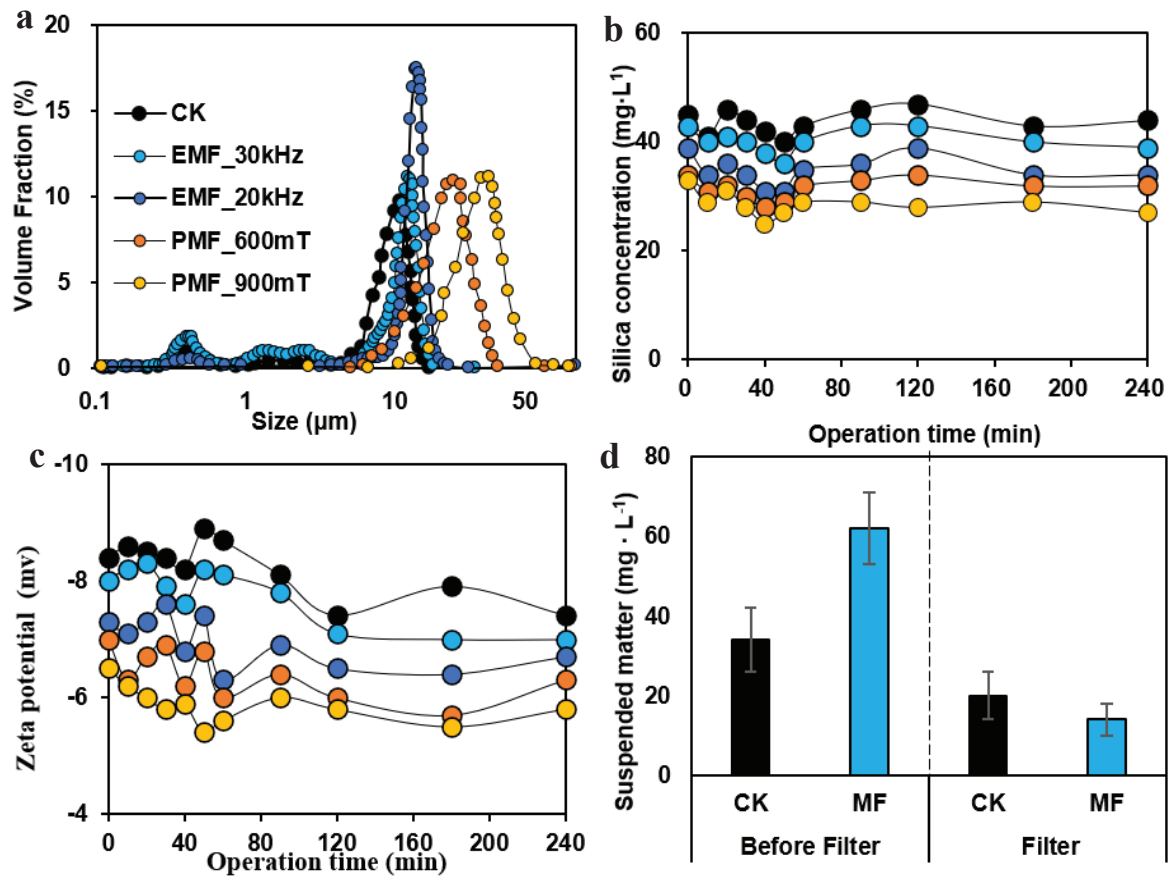
Fig. 7. Effects of MF on suspended matter, silica concentration and particle size

(a)　Particle size, (b) Silica concentration, (c) Zeta potential, (d) Suspended solids under filter / before filter

Table.1 Water quality parameter

Parameters	Results	Parameters	Results
pH	7.7 +/- 0.6	Bicarbonate ion (mg L^{-1})	483.6 +/- 19.2
suspended solids (mg L^{-1})	38.2 +/- 5.3	Sulfate anion (mg L^{-1})	641.3 +/- 21.3
electrical conductivity (dS m^{-1})	2.64 +/-0.06	Chloridion (mg L^{-1})	442.2 +/- 15.9
Potassium ion (mg L^{-1})	47.6 +/- 2.04	Phosphorus ion (mg L^{-1})	46.1 +/- 5.6
Sodium ion (mg L^{-1})	521 +/- 13.5	Iron ion (mg L^{-1})	12.4 +/- 3.1
Magnesium ion (mg L^{-1})	83.4 +/- 5.7	Calcium ion (mg L^{-1})	191.2 +/- 10.3
Temperature (℃)	27 +/- 6.7	Oxidation reduction potential (mv)	79 +/- 3.2
Silica concentration (mg L^{-1})	40 +/- 5.8	Surface Tension (m N m^{-1})	52 +/- 2.3
Zeta potential (mv)	-7 +/- 1.3		
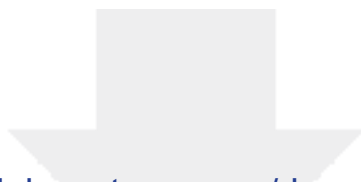
Click here to access/download
Supplementary material for on-line publication only
Supplementary information.docx

Author contributions

Zeyuan Liu: Writing - Original Draft, Investigation, Formal analysis, Data Curation

Marco Di Luccio: Review & Editing, Investigation, Validation

Sergio García: Review & Editing, Investigation, Validation

Jaume Puig-Bargués: Writing - Review & Editing

Zhao Xiao: Writing - Review & Editing

Alfredo Trueba: Resources, Review & Editing

Tahir Muhammad: Resources, Review & Editing

Yang Xiao: Writing - Review & Editing

Yunkai Li: Writing - Review & Editing, Conceptualization, Methodology, Resources, Supervision, Project administration, Funding acquisition